Supplementary Information

Branch-like Mo-doped Ni_3S_2 nanoforest as high-efficiency and durable catalyst for overall urea electrolysis

Han Xu,† Yu Liao,† Zhifei Gao, Yan Qing, Yiqiang Wu, and Liaoyuan Xia*

Hunan Province Key Laboratory of Materials Surface & Interface Science and Technology, College of Material Science and Engineering, Central South University of Forestry and Technology, Changsha 410004, P. R. China

E-mail: xly1516@126.com (L.Y. Xia)

† These authors contributed equally to this work.

Section 1. Theoretical calculation

1.1 Computation details. All DFT computations were carried out using the Vienna ab initio simulation package (VSVP). The ion-electron interactions were described by using the projector augmented wave (PAW) method. The exchange-correlation energy was evaluated by the generalized gradient approximation (GGA) with Perdew-Burke-Ernzerhof (PBE) function. The cut-off energy was set to 400 eV for plane wave expansion. Furthermore, the Brillouin zone was sampled by (4×3×1) Monkhorst-Pack K-point grid, and a vacuum space of 12 Å was placed along Z axis to avoid the interaction among the slabs. In the slab calculations, the atoms on the top layer of the slab could relax during the optimization of overall adsorption structure, and the other atoms were immobilized. The atomic relaxation will be stopped as soon as the total energy tolerance was converged to 10^{-5} eV and the changes of the force on atoms less than 0.01 eV/Å.

1.2 Slab models for (110) facet of Ni_3S_2 and Mo-doped Ni_3S_2. According to the XRD patterns and HRTEM images of the samples, we particularly chosen the (110) facet of Ni_3S_2 and Mo-doped Ni_3S_2 for further computations discussions. The Ni_3S_2 (110) surface was constructed by cleaving the optimized bulk structure through the corresponding planes (Fig. S6a). In this model, one Ni atom was randomly replaced by Mo atom, which formed the model of Mo-doped Ni_3S_2 (Fig. S6b).

1.3 The free-energy computations of NH_2* and CO* adsorption during UOR. The key intermediates during the UOR should be NH_2* and CO*, and these key adsorbates are formed through the following reaction, wherein * represent the adsorbed intermediate on the surface:

$$CO(NH_2)_{2(aq)} \rightarrow CO(NH_2)_2* \quad \text{(S1)}$$

$$CO(NH_2)_2* \rightarrow CO* + 2NH_2* \quad \text{(S2)}$$

$$CO* + 2OH^- \rightarrow CO_{2(g)} + H_2O_{(l)} + 2e^- \quad \text{(S3)}$$

$$2NH_2* + 4OH^- \rightarrow N_{2(g)} + 4H_2O_{(l)} + 4e^- \quad \text{(S4)}$$

In the UOR process, based on post-processing experiment and characterization results, an in-situ surface conversion of Ni_3S_2 into NiOOH takes place during UOR. Thus, the Mo-doped Ni_3S_2 are mimicked by an adsorbed doping metal atom on NiOOH. We studied the structures and energetics of the molecular and dissociative adsorption of urea on NiOOH and Mo-doped NiOOH surface. Fig. S11 present several stable configurations of urea molecular and dissociative adsorption, respectively. The adsorption free energy (ΔG) was calculated as the description to evaluate the UOR performance of various catalysts and using the following equation (Eqn. S5).

$$\Delta G = \Delta E_{ads} + \Delta E_{ZPE} - T\Delta S \qquad (S5)$$

Where ΔE_{ads} is the adsorption energy defined as the electronic energy difference; T is the temperature (T=298.15 K), ΔE_{ZPE} and ΔS are the contributions to the free energy from the zero-point vibration energy and entropy, respectively.

Section 2. Figures and curves

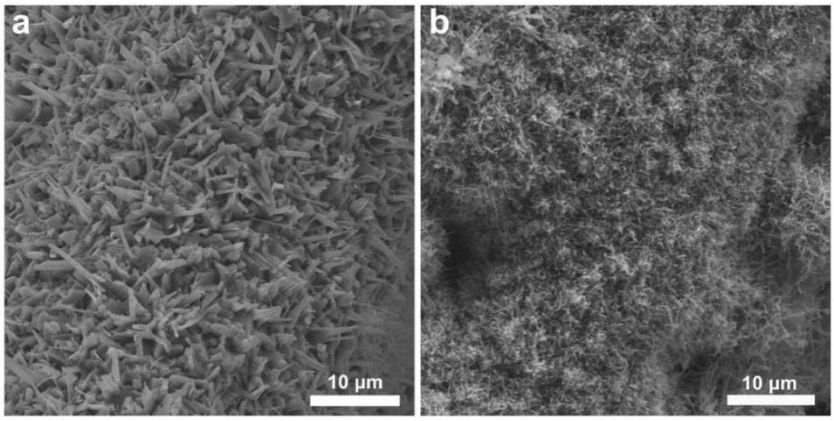

Fig. S1. SEM images of (a) Ni_3S_2 and (b) Mo-doped Ni_3S_2.

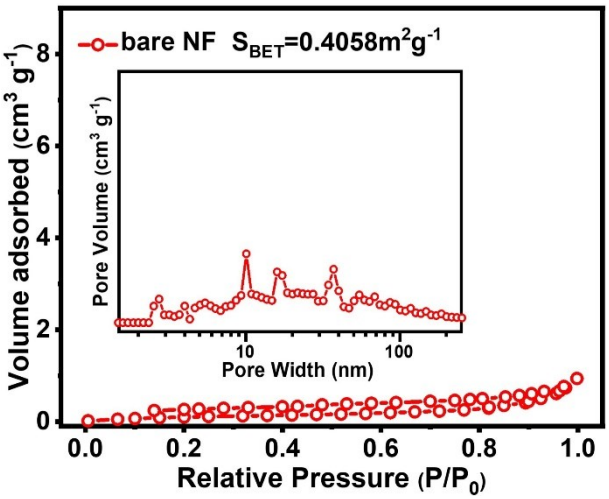

Fig. S2. Adsorption/desorption isotherms of bare Ni foam (the inset shows the corresponding pore size distribution pattern).

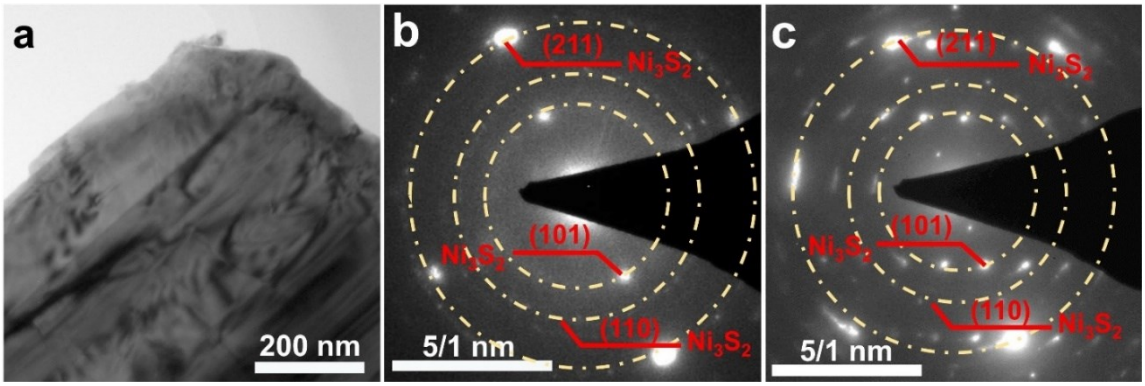

Fig. S3. (a) TEM image of Ni_3S_2. SAED patterns of (b) Mo-doped Ni_3S_2 and (c) Ni_3S_2, respectively.

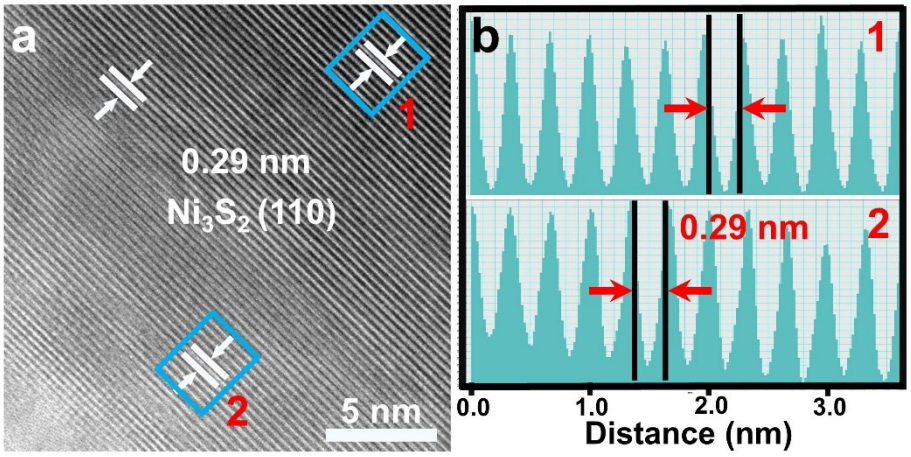

Fig. S4. (a) HRTEM image of Ni_3S_2. (b) The lattice spacing corresponding to the selected areas in panel (a).

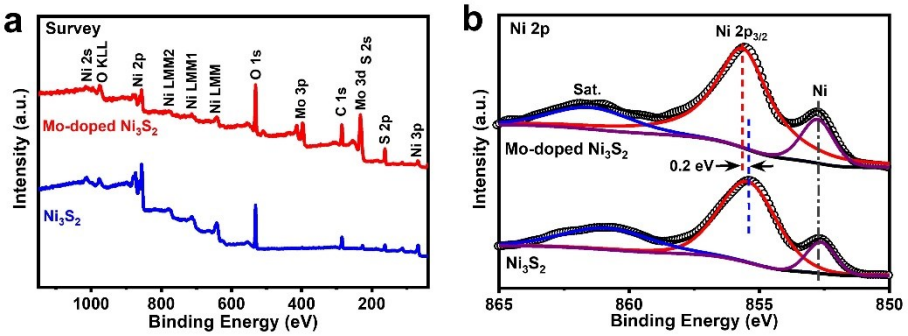

Fig. S5. (a) XPS survey pattern of obtained samples. (b) The high-resolution Ni 2p spectra.

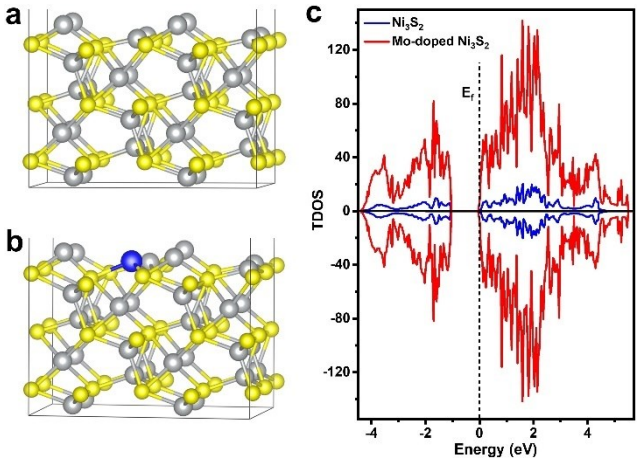

Fig. S6. Theoretical structure models of (a) pure Ni_3S_2 and (b) Mo-doped Ni_3S_2. (c) The calculated total density of states for pure Ni_3S_2 and Mo-doped Ni_3S_2. (The yellow, gray and blue balls represent the sulfur, nickel and molybdenum atoms, respectively)

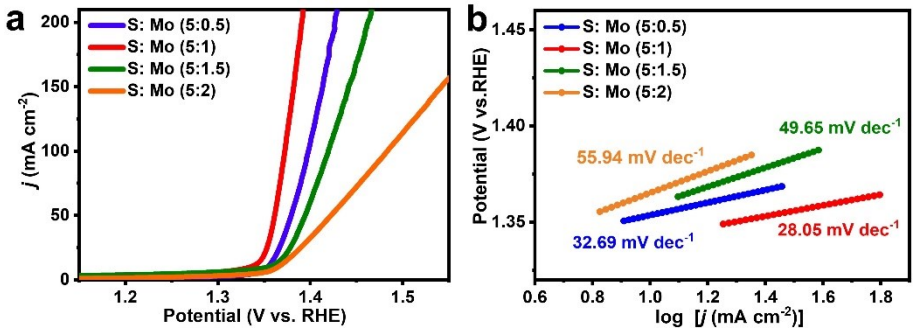

Fig. S7. (a) LSV curves of Mo-doped Ni_3S_2 with different S/Mo molar ratio in 1.0 M KOH with 0.3 M urea, (b) the corresponding Tafel slopes.

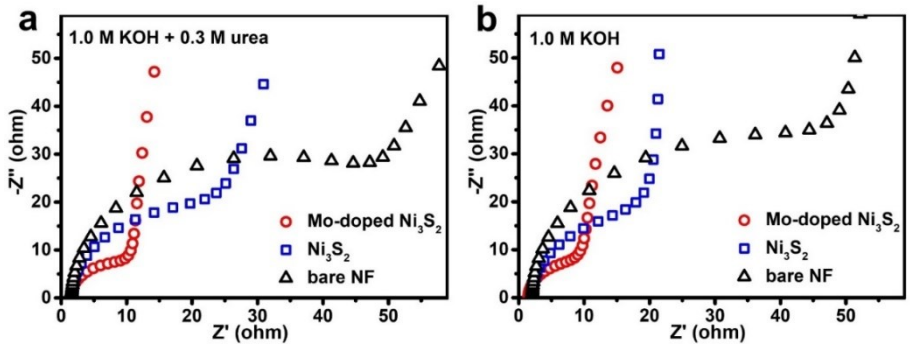

Fig. S8. Nyquist plots of Mo-doped Ni_3S_2 in 1.0 M KOH (a) with 0.3 M urea and (b) without urea.

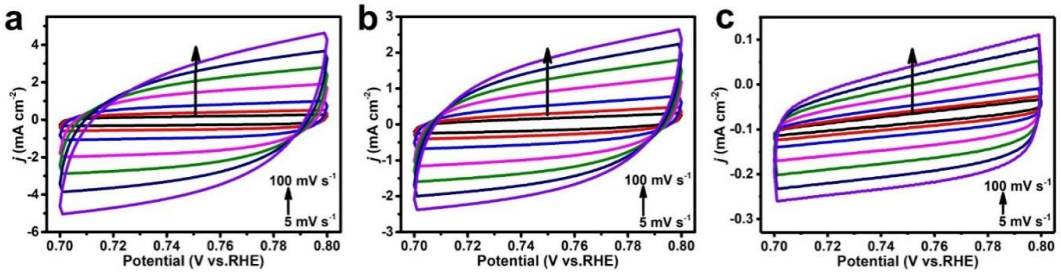

Fig. S9. Cyclic voltammograms curves of (a) Mo-doped Ni_3S_2, (b) Ni_3S_2, and (c) bare NF obtained at 0.7~0.8 V (*vs.* RHE) with various scan rates (in the direction as indicated by the arrow: 5, 10, 20, 40, 60, 80 and 100 mV s^{-1}) in 1.0 M KOH with 0.3 M urea.

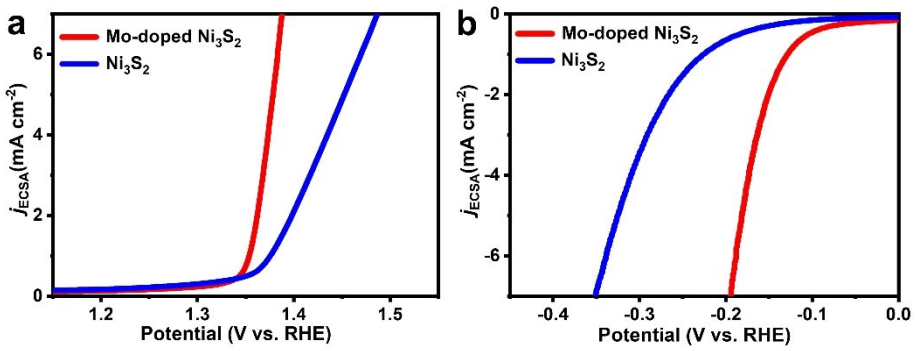

Fig. S10. (a) UOR and (b) HER polarization curves of Mo-doped Ni_3S_2 and Ni_3S_2 normalized by the ECSA.

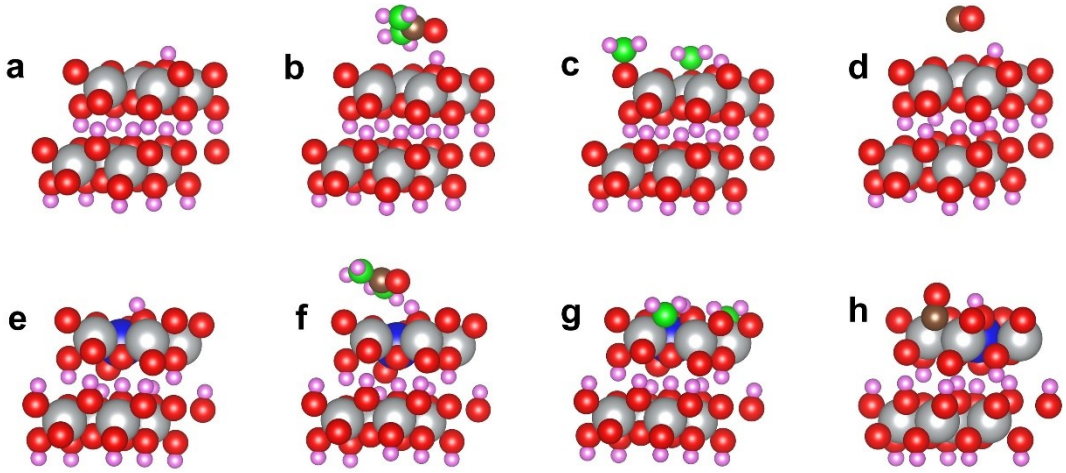

Fig. S11. Optimized structure of urea molecular dissociative adsorption on (a, b, c, d) NiOOH surface and (e, f, g, h) Mo-doped NiOOH surface (The gray and blue balls represent the nickel and molybdenum atoms, respectively. The brown, green, brown, red and pink balls represent the carbon, nitrogen, oxygen and hydrogen atoms, respectively).

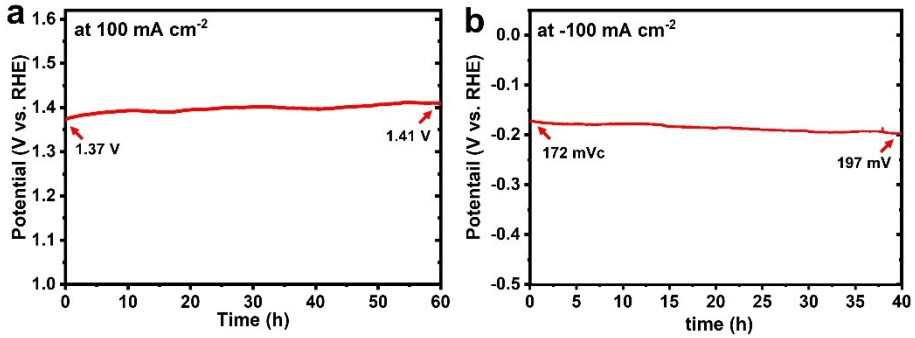

Fig. S12. (a) UOR and (b) HER long-time stability test of Mo-doped Ni_3S_2 at a constant current density of 100 mA cm^{-2} and -100 mA cm^{-2}, respectively.

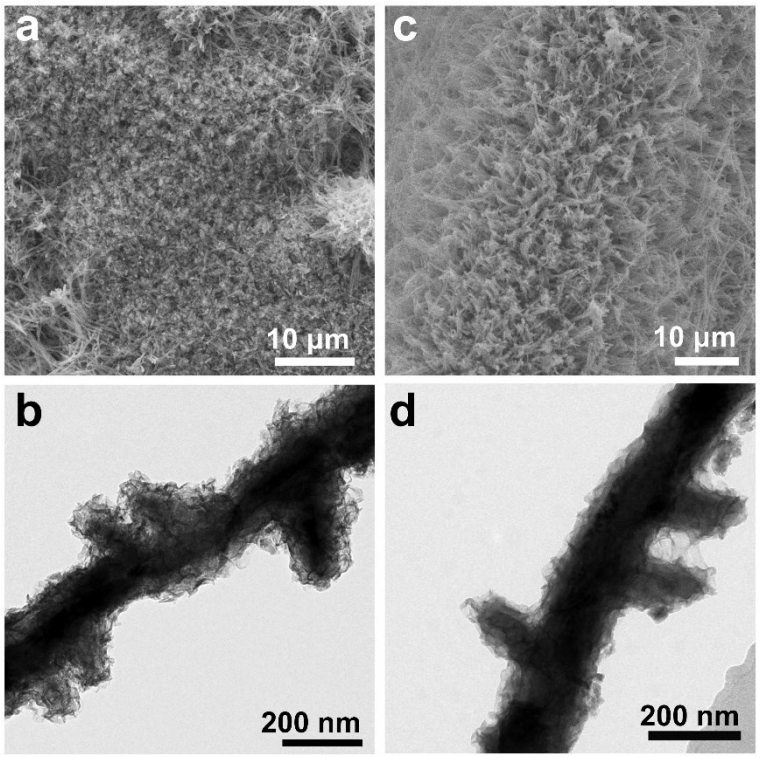

Fig. S13. SEM and TEM images of Mo-doped Ni_3S_2 after (a, b) UOR and (c, d) HER long-term stability test.

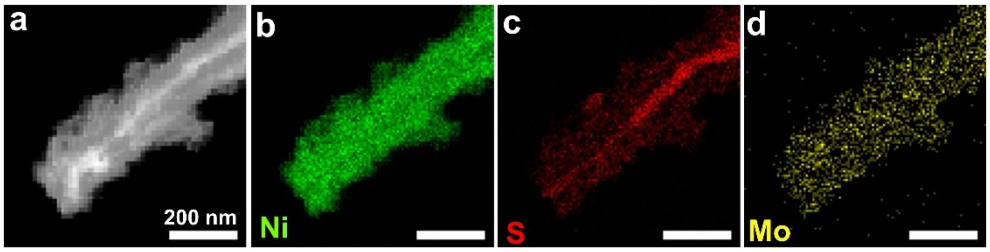

Fig. S14. (a) STEM image and (b-d) the corresponding element mappings of the Mo-doped Ni_3S_2 after UOR long-time stability test.

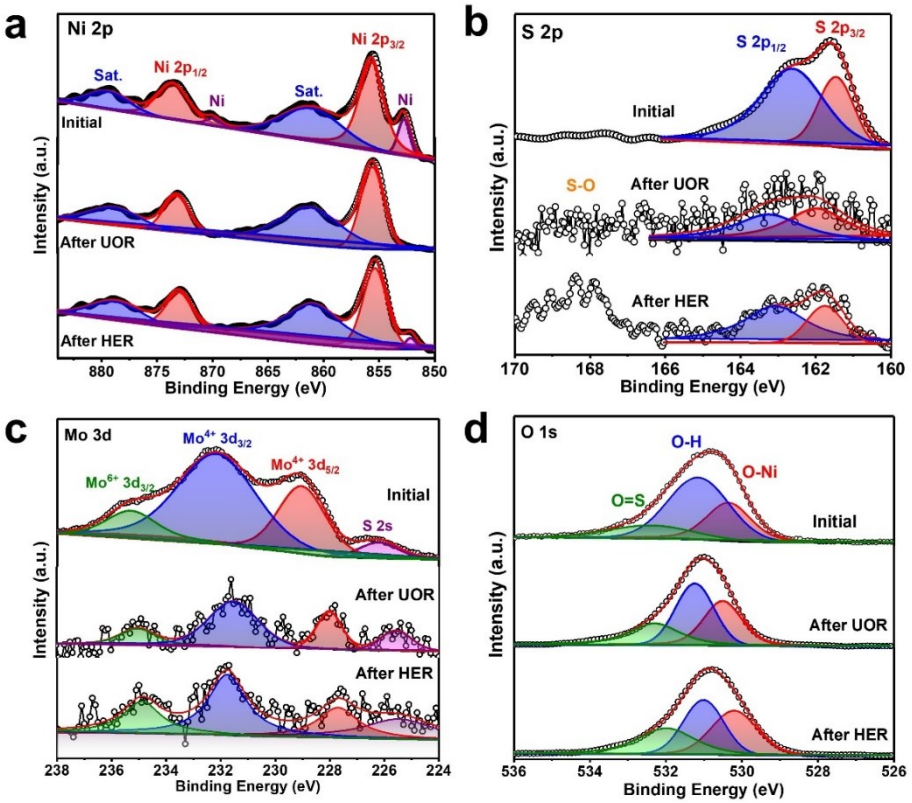

Fig. S15. (a) Ni 2p, (b) S 2s, (c) Mo 3d and (d) O 1s high-resolution XPS spectra of Mo-doped Ni_3S_2 before and after UOR and HER test.

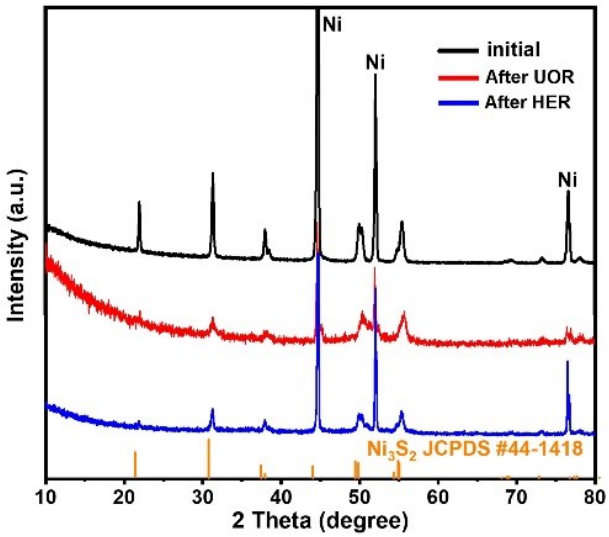

Fig. S16. XRD patterns of Mo-doped Ni_3S_2 after UOR and HER stability test.

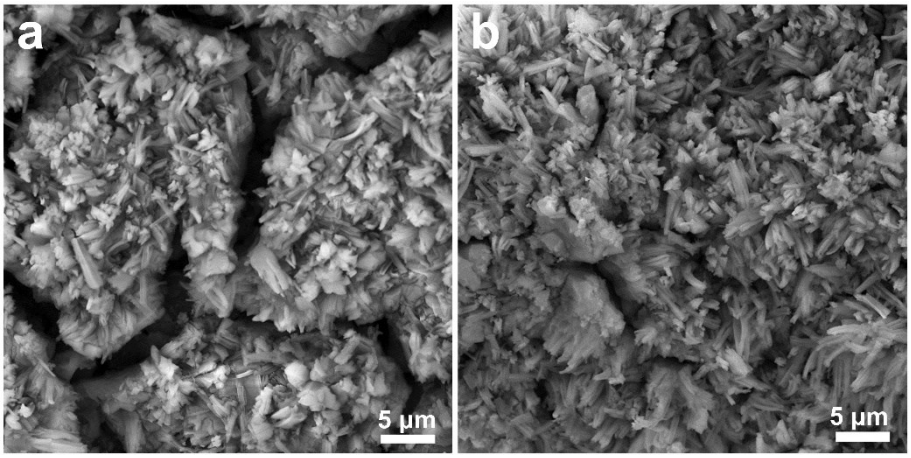

Fig. S17. SEM images the Ni_3S_2 after (a) UOR and (b) HER stability test.

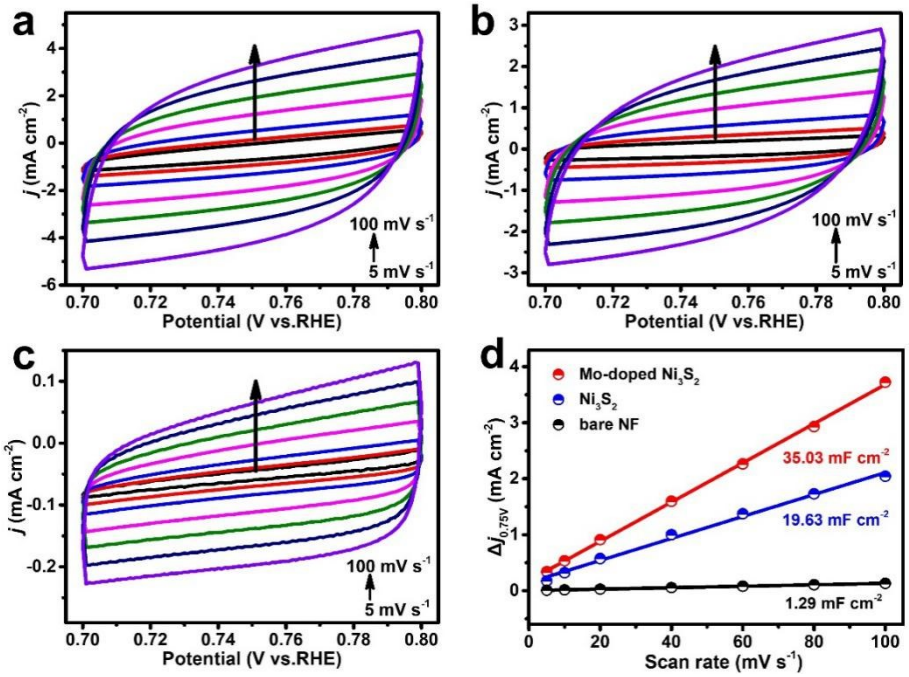

Fig. S18. Cyclic voltammograms curves of (a) Mo-doped Ni_3S_2, (b) Ni_3S_2, and (c) bare NF obtained at 0.7~0.8 V (*vs.* RHE) with various scan rates (in the direction as indicated by the arrow: 5, 10, 20, 40, 60, 80 and 100 mV s^{-1}) in 1.0 M KOH. (d) Plots of capacitive currents as a function of scan rate for different catalysts.

Section 3. Tables

Table S1. Comparison of UOR performance for Mo-doped Ni_3S_2 with various recently reported electrocatalysts.

Catalytic material	Electrolyte	Potential (V *vs.* RHE)	Tafel slope (mV dec^{-1})	References
Mo-doped Ni_3S_2	1.0 M KOH 0.3 M urea	1.33 @ 10 mA cm^{-2} 1.37 @ 100 mA cm^{-2}	28.05	This Work
Pt/C	1.0 M KOH 0.3 M urea	1.37 @ 10 mA cm^{-2} 1.45 @ 100 mA cm^{-2}	35.44	This Work
Ni_3Se_4 nanorod/NF	1.0 M KOH 0.5 M urea	1.38@10 mA cm^{-2} ~1.44@100 mA cm^{-2}	N.A.	*J. Mater. Chem. A*., **2018**, 6, 15653
Ni-Mo nanotube/NF	1.0 M KOH 0.1 M urea	1.36@10 mA cm^{-2} ~1.42@100 mA cm^{-2}	55	*Nano Energy*, **2019**, 60, 894
NiMoO-Ar/NF	1.0 M KOH 0.5 M urea	1.37@ 10 mA cm^{-2} 1.42 @ 100 mA cm^{-2}	19	*Energy Environ. Sci*., **2018**, 11, 1890
Ni/C	1.0 M KOH 0.33 M urea	~1.38@10 mA cm^{-2} 2.0@ 100 mA cm^{-2}	N.A.	*ACS Appl. Mater. Interfaces*, **2018**, 10, 4750
$MnO_2/MnCo_2O_4$/Ni	1.0 M KOH 0.5 M urea	~1.37@10 mA cm^{-2} ~1.47@ 100 mA cm^{-2}	72	*J. Mater. Chem. A*., **2017**, 5, 7825
NF@p-Ni	1.0 M KOH 0.33 M urea	~1.38@10 mA cm^{-2} ~1.57@100 mA cm^{-2}	N.A.	*Electrochim. Acta*, **2019**, 304, 131
Ni-MOF/NF	1.0 M KOH 0.5 M urea	1.37@10 mA cm^{-2} ~1.56@100 mA cm^{-2}	N.A.	*Chem. Commun*., **2017**, 53, 10906
$Ni(OH)_2$NS@NW/NF	1.0 M KOH 0.33 M urea	1.40@10 mA cm^{-2} N.A.	47	*Electrochim. Acta*, **2018**, 268, 211
$Fe_{11.1\%}$-Ni_3S_2/Ni foam	1.0 M KOH 0.33 M urea	~1.35@10 mA cm^{-2} 1.39@100 mA cm^{-2}	N.A.	*J. Mater. Chem. A,* **2018**, 6, 4346
SL $Ni(OH)_2$ NS/CC	1.0 M KOH 0.33 M urea	~1.37@10 mA cm^{-2} ~1.40@100 mA cm^{-2}	N.A.	*J. Mater. Chem. A*., **2018**, 6, 13867

Table S2. List of C_{dl} values of bare NF, Ni_3S_2 and Mo-doped Ni_3S_2.

Catalytic material	C_{dl} (mF cm^{-2}) for UOR	C_{dl} (mF cm^{-2}) for HER
bare NF	1.28	1.29
Ni_3S_2	17.73	19.63
Mo-doped Ni_3S_2	33.51	35.03

Table S3. Comparison of UOR intrinsic activity for Mo-doped Ni_3S_2 with several recently reported earth-abundant transition-metal-based electrocatalysts in the alkaline media.

Catalytic material	Mass loading (mg cm^{-1})	j_{ECSA}(mA cm^{-1})	Potential (V vs. RHE)	References
Mo-doped Ni_3S_2	12	2	1.36	This Work
Ni_3Se_4 nanorod/NF	1.0	2	1.41	*J. Mater. Chem. A*., **2018**, 6, 15653
NiMoO-Ar/NF	5.1	2	1.38	*Energy Environ. Sci*., **2018**, 11, 1890
FQD/CoNi-LDH/NF	0.98	2	1.42	*Chem. Eng. J., 2020, **390**, 124525*
NiTe/rGO/NF	3.0	2	1.40	*ACS Appl. Energy Mater., 2019, **2**, 3363*
$MnCo_2O_{4.5}$@$Ni(OH)_2$/NF	N.A.	2	1.37	*Chem. Eng. J.*, **2020**, 381, 122603

Table S4. Comparison of HER performance for Mo-doped Ni_3S_2 with various recently reported electrocatalysts in the alkaline media (1.0 M KOH).

Catalytic material	Substrate	Overpotential (mV)	Tafel slope (mV dec^{-1})	Reference
Mo-doped Ni_3S_2	Ni foam	90 @ -10 mA cm^{-2} 172@ -100 mA cm^{-2}	81.66	This Work
Pt/C	Ni foam	15@ -10 mA cm^{-2} 77@ -100 mA cm^{-2}	28.8	This Work
CoMoNiS-NF-31	Ni foam	113 @ -10 mA cm^{-2} N.A.	85	*J. Am. Chem. Soc.*, **2019**, 141, 10417
Ni_3S_2@MoS_2/FeOOH	Ni foam	95 @ -10 mA cm^{-2} ~170 @ -100 mA cm^{-2}	85	*Appl. Catal. B: Environ.*, **2019**, 244, 1004
Ni_3S_2@MoS_x/NiO	Ni foam	118 @ -10 mA cm^{-2} ~260 @ -100 mA cm^{-2}	65	*J. Mater. Chem. A*., **2018**, 6, 20491
Fe-MoS_2/Ni_3S_2/NF-2	Ni foam	130.6 @ -10 mA cm^{-2} ~290 @ -100 mA cm^{-2}	112.7	*Dalton Trans.*, **2019**,48, 12186
Ni_{SA}-MoS_2	carbon cloth	98 @ -10 mA cm^{-2} N.A.	75	*Nano Energy*, **2018**, 53, 458
(Ni, Fe)S_2@MoS_2	carbon cloth	130 @ -10 mA cm^{-2} ~280 @ -100 mA cm^{-2}	101.22	*Appl. Catal. B: Environ.*, **2019**, 247, 107
MoS_2−Ni_3S_2 HNRs	Ni foam	98 @ -10 mA cm^{-2} ~190 @ -100 mA cm^{-2}	61	*ACS Catal*., **2017**, 7, 2357
MoS_2/Ni_3S_2 Heterostructures	Ni foam	110 @ -10 mA cm^{-2} N.A.	83.1	*Angew. Chem. Int. Edit*., **2016**, 55, 6702
Co_9S_8/Ni_3S_2	Ni foam	128 @ -10 mA cm^{-2} ~220 @ -100 mA cm^{-2}	97.6	*Appl. Catal. B: Environ.*, **2019**, 253, 246
$Fe_{11.1\%}$-Ni_3S_2/Ni foam	Ni foam	126@ -10 mA cm^{-2} ~240 @ -100 mA cm^{-2}	89	*J. Mater. Chem. A*, **2018**, 6, 4346

Table S5. Comparison of HER intrinsic activity for Mo-doped Ni_3S_2 with several recently reported earth-abundant transition-metal-based electrocatalysts in the alkaline media.

Catalytic material	Mass loading (mg cm^{-2})	j_{ECSA}(mA cm^{-1})	Overpotential (mV)	Reference
Mo-doped Ni_3S_2	12	2	152	This Work
δ-FeOOH/Ni_3S_2/NF	2.5	2	170	*J. Mater. Chem. A*., **2020**, 8, 21199
$Ni(OH)_2$-$NiMoO_x$/NF	N.A.	2	＞200	*Adv. Energy Mater.,* **2019**, 9, 1902703
CoP/NPC/TF	1.5	2	160	*Adv. Energy Mater.,* **2019**, 0, 1803970
MoS_2−Ni_3S_2 HNRs	13	2	175	*ACS Catal*., **2017**, 7, 2357
Mo-Ni_3S_2/Ni_xP_y	3.15	2	＞160	*Adv Energy Mater.,* **2020**, 10, 1903891.

Table S6. Comparison of the overall urea-electrolysis efficiency for Mo-doped Ni_3S_2 with other newly-reported highly active bifunctional catalysts.

Catalytic material	Electrolyte	Voltage @10 mA cm^{-2} (V)	Operation time	Reference
Mo-doped Ni_3S_2	1.0 M KOH 0.3 M urea	1.45	120 h	This Work
HC-NiMoS/Ti	1.0 M KOH 0.5 M urea	1.59	10 h	*Nano Research*, **2018**, 11, 988
Ni/C	1.0 M KOH 0.33 M urea	1.60	12 h	*ACS Appl. Mater. Inter*., **2018**, 10, 4750
Ni-Mo nanotube	1.0 M KOH 0.1 M urea	1.43	10 h	*Nano Energy*, **2019,** 60, 894
MnO_2/$MnCo_2O_4$/Ni	1.0 M KOH 0.5 M urea	1.55	15 h	*J. Mater. Chem. A*, **2017**, 5, 7825
NiCoFe LDH/NF	1.0 M KOH 0.33 M urea	1.49	50 h	*ACS Sustain. Chem. Eng*., **2019**, 7, 10035
CoMn/$CoMn_2O_4$	1.0 M KOH 0.5 M urea	1.51	15 h	*Adv. Funct. Mater.*, **2020,** 2000556
$Fe_{11.1\%}$-Ni_3S_2/Ni foam	1.0 M KOH 0.5 M urea	1.46	22 h	*J. Mater. Chem. A*, **2018**, 6, 4346
$NiCo_2S_4$ NS/CC	1.0 M KOH 0.33 M urea	1.49	20 h	*ACS Sustain. Chem. Eng*., **2018**, 6, 5011
CoS_2/Ti mesh	1.0 M KOH 0.3 M urea	1.59	~ 4.2 h	*Electrochim. Acta*, **2017**, 246, 776
1%Cu:α-$Ni(OH)_2$/NF	1.0 M KOH 0.33 M urea	1.49	40 h	*J. Mater. Chem. A*, **2019**, 7, 13577